

A squeezed-state primer

Richard W. Henry

TRW Space and Technology Group, One Space Park, Redondo Beach, California 90278 and Department of Physics, Bucknell University, Lewisburg, Pennsylvania 17837

Sharon C. Glotzer

TRW Space and Technology Group, One Space Park, Redondo Beach, California 90278

(Received 19 February 1987; accepted for publication 30 June 1987)

Using only elementary quantum-mechanical concepts, the statistical properties of various harmonic oscillator states that are linear superpositions of its energy eigenfunctions are described. These superpositions include coherent states and squeezed (or two-photon coherent) states. The resulting Gaussian, minimum-uncertainty wave packets are shown to oscillate back and forth for both coherent and squeezed states, but with an oscillating "width" for the squeezed states. Also examined are the principles underlying the production of squeezed electromagnetic waves via parametric amplification or four-wave mixing, their measurement by homodyne detection, and the connection between squeezing and non-Poissonian counting statistics.

I. INTRODUCTION

Squeezed states of the electromagnetic field have received increasing theoretical attention¹⁻¹⁴ during the last few years, and recently several laboratories have obtained experimental evidence of squeezed states produced by various nonlinear processes.¹⁵⁻¹⁹ Squeezed states give promise of measurement results better than those normally expected from the Heisenberg uncertainty principle, especially in connection with optical interferometers used to measure the relative positions of gravity-wave detectors²⁰ and in optical communications.^{21,22} Despite all this attention by researchers, there has not yet appeared a tutorial article on squeezed states that develops physical models from elementary principles at a level accessible to nonspecialists. We hope that this article will fill that gap in the literature of squeezed states.

The electromagnetic radiation in each standing-wave mode in a cavity resonator has been shown²³ to be analogous to a harmonic oscillator. The oscillator's displacement x can be taken to correspond to the radiation mode's electric field and then the oscillator's momentum p corresponds to the mode's magnetic field. Just as the position and momentum of the oscillator are 90° out of phase in time, so are the electric and magnetic fields of the radiation mode 90° out of phase in time at each point in space. The energy of the oscillator sloshes back and forth between potential and kinetic, just as the energy of the standing-wave field sloshes back and forth between electric and magnetic. (Notice that we are dealing with a *standing wave*; for a traveling wave the electric and magnetic fields are in phase.) The familiar quantization of the oscillator's total energy corresponds to having only an integral number of photons in the radiation mode.

We will describe squeezed states quantum mechanically, in terms of linear combinations (superpositions) of harmonic oscillator energy eigenfunctions. For certain linear combinations, known as *coherent states*,²⁴ the variances (squares of the uncertainties) of position and momentum are constant in time and their product equals the minimum value allowed by the Heisenberg uncertainty principle. But, for the linear combinations that produce squeezed states, the variances of the position and momentum oscil-

late in time 180° out of phase with one another and at twice the oscillator frequency. And, at any instant of time, *one of the variances can be smaller than the square root of the minimum-uncertainty product.*

Squeezed oscillator states are analogous to the following classical situation. Imagine an ensemble of identical oscillators (same resonant frequency) all having nearly the same displacement from equilibrium, x_0 , at $t = 0$ but having a very wide distribution of momenta. A quarter cycle later, we would find a very wide distribution of displacements due to the wide range of initial momenta. But, after one-half cycle, we would again find all the oscillators grouped on the other side of the equilibrium position, near $-x_0$. The uncertainty in displacement has undergone an oscillation. The only difference in quantum mechanics is that if all the oscillators had nearly the same initial displacement, then their initial momenta would *necessarily* be spread over a wide range, consistent with the Heisenberg uncertainty principle.

We begin by reviewing the harmonic oscillator eigenfunctions (number states) and the annihilation and creation operators in Sec. II. Section III deals with linear combinations of number states and shows that the coefficients characterizing these linear combinations rotate in the complex plane. We also show how the complex rotating phasors used to describe a classical oscillator are related to the annihilation and creation operators. In Sec. IV we define the coherent states to be eigenfunctions of the annihilation operator, find their number state coefficients, and show that the coherent states are minimum-uncertainty states in the sense of the Heisenberg uncertainty principle.

Section V introduces squeezed states as eigenfunctions of a new quantum-mechanical operator, which is a linear combination of the annihilation and creation operators, and shows that squeezed states are characterized by oscillating variances. Section VI then describes how squeezed states can be generated through nonlinear processes such as parametric amplification and four-wave mixing. In Sec. VII we demonstrate how homodyne detection can produce a squeezed measurement with a nonoscillating uncertainty that is smaller than the usual uncertainty principle limit. Section VIII concludes with a summary and some additional comments about squeezed states and the utility of our methodology.

II. REVIEW OF HARMONIC OSCILLATOR ENERGY EIGENFUNCTIONS

Our entire discussion is based on the set of orthonormal energy eigenfunctions of the harmonic oscillator, $\psi_n(x)$, $n = 0, 1, 2, \dots$. These are derived in most quantum mechanics texts,²⁵ beginning with the time-independent Schrödinger equation. The energy eigenfunctions are also called number states and represented by a Dirac ket, $|n\rangle$, to denote the fact that a number state has a definite number of quanta of energy.

From the freedom to define the magnitudes of three mechanical "units," we can set $\hbar/2\pi$, the oscillator mass m , and its spring constant k , all equal to 1. In these units, the number states, each a product of a fixed-width Gaussian and a Hermite polynomial, $H_n(x)$, are

$$\psi_n(x) = 2^{-n/2} (n!)^{-1/2} \pi^{-1/4} \exp(-x^2/2) H_n(x), \quad (1)$$

where the $H_n(x)$ are defined recursively by

$$\begin{aligned} H_0(x) &= 1, \\ H_1(x) &= 2x, \\ H_n(x) &= 2xH_{n-1}(x) - 2(n-1)H_{n-2}(x). \end{aligned} \quad (2)$$

We may think of Eqs. (1) and (2) as establishing the connection between the x representation of a quantum state, i.e., the wave packet, and the n representation. In Dirac notation, $\psi_n(x)$ is equivalent to $\langle x|n\rangle$, where the bracket indicates the "projection" of the number state into the x representation. While either representation contains complete information about the state, in subsequent sections we will generally define our states in the n representation, i.e., in terms of the contributions from the various number states, and then convert to the x representation via Eqs. (1) and (2) to acquire physical insight.

We are primarily interested in computing the uncertainties in the oscillator's position and momentum for the number states and for various linear combinations of number states. These uncertainties are best characterized by the mean-square deviations from the average, or variances:

$$\text{var}(x) = \langle x^2 \rangle - \langle x \rangle^2 \quad (3)$$

and

$$\text{var}(p) = \langle p^2 \rangle - \langle p \rangle^2, \quad (4)$$

where the symbol $\langle \rangle$ denotes the quantum-mechanical ensemble average, or expectation value.

If we know an oscillator's full position- and time-dependent wavefunction $\psi(x,t)$, we can calculate these average values (which, in general, depend on time, as we will discuss in more detail later) by means of integrals such as

$$\langle x \rangle = \int_{-\infty}^{\infty} \psi^*(x,t) x \psi(x,t) dx \quad (5)$$

and

$$\langle p \rangle = \int_{-\infty}^{\infty} \psi^*(x,t) \left(-i \frac{d}{dx} \psi(x,t) \right) dx. \quad (6)$$

Here, $\psi^*(x,t)$ is the complex conjugate of $\psi(x,t)$ and $-i(d/dx)$ represents the momentum operator \hat{p} in the x representation.

The integrals for $\langle x \rangle$, $\langle x^2 \rangle$, $\langle p \rangle$, and $\langle p^2 \rangle$, needed to calculate $\text{var}(x)$ and $\text{var}(p)$, are tedious to carry out; another method, due to Dirac,²⁶ in which we calculate in the n representation rather than the x representation, is pre-

ferred. In Dirac's method we work entirely with new operators called annihilation and creation operators, \hat{a} and \hat{a}^+ . These operators are defined in terms of the position and momentum operators by

$$\hat{a} \equiv (\hat{x} + i\hat{p})/\sqrt{2} \quad (7)$$

and the Hermitian conjugate

$$\hat{a}^+ \equiv (\hat{x} - i\hat{p})/\sqrt{2}. \quad (8)$$

Dirac showed that \hat{a} operating on any number state $|n\rangle$ gives \sqrt{n} times the next *lower* state $|n-1\rangle$ and \hat{a}^+ operating on any number state gives $\sqrt{n+1}$ times the next *higher* state $|n+1\rangle$. That is,

$$\hat{a}|n\rangle = \sqrt{n}|n-1\rangle \quad (9)$$

and

$$\hat{a}^+|n\rangle = \sqrt{n+1}|n+1\rangle. \quad (10)$$

The terms "creation" and "annihilation" come from the fact that \hat{a}^+ produces a state with one more quantum of energy, while \hat{a} produces a state with one less.

These operators have the additional properties

$$\hat{a}^+ \hat{a} |n\rangle = n |n\rangle \quad (11)$$

and

$$\hat{a} \hat{a}^+ - \hat{a}^+ \hat{a} = 1, \quad (12)$$

which may be demonstrated by repeated use of the creation and annihilation properties described in Eqs. (9) and (10). Notice that in Eq. (12) we have not written a ket; all number states and, therefore, *all linear combinations of number states* are eigenfunctions of $(\hat{a} \hat{a}^+ - \hat{a}^+ \hat{a})$ with eigenvalue unity.

To calculate the averages needed to find the variances of x and p for any state, we first solve Eqs. (7) and (8) for the position and momentum operators:

$$\hat{x} = (\hat{a} + \hat{a}^+)/\sqrt{2}, \quad (13)$$

$$\hat{p} = (\hat{a} - \hat{a}^+)/i\sqrt{2}. \quad (14)$$

By squaring (13) and (14) we can express operators \hat{x}^2 and \hat{p}^2 as

$$\hat{x}^2 = (\hat{a}^+ \hat{a} + \hat{a} \hat{a}^+ + \hat{a} \hat{a} + \hat{a}^+ \hat{a}^+)/2 \quad (15)$$

and

$$\hat{p}^2 = (\hat{a}^+ \hat{a} + \hat{a} \hat{a}^+ - \hat{a} \hat{a} - \hat{a}^+ \hat{a}^+)/2. \quad (16)$$

The integral expressions for the averages are then replaced with Dirac brackets; for example,

$$\langle x \rangle = \langle \psi | \hat{x} | \psi \rangle = \langle \psi | [(\hat{a} + \hat{a}^+)/\sqrt{2}] | \psi \rangle \quad (17)$$

and

$$\langle p \rangle = \langle \psi | \hat{p} | \psi \rangle = \langle \psi | [(\hat{a} - \hat{a}^+)/i\sqrt{2}] | \psi \rangle. \quad (18)$$

From (17) and (18) we can deduce that if ψ is a number state, then the average position and momentum are zero. This is because $\hat{a} \pm \hat{a}^+$ operates on $|n\rangle$ to produce linear combinations of $|n-1\rangle$ and $|n+1\rangle$ and because the scalar products $\langle n|n-1\rangle$ and $\langle n|n+1\rangle$ are zero by orthogonality.

The variances of the number states are not, however, zero. From Eq. (15) we have

$$\langle x^2 \rangle = \langle n | [(\hat{a}^+ \hat{a} + \hat{a} \hat{a}^+ + \hat{a} \hat{a} + \hat{a}^+ \hat{a}^+)/2] | n \rangle. \quad (19)$$

Using Eqs. (11) and (12), we can combine the first two operators in (19) to give

$$\hat{a}^+ \hat{a} + \hat{a} \hat{a}^+ = 2\hat{a}^+ \hat{a} + 1 = 2n + 1. \quad (20)$$

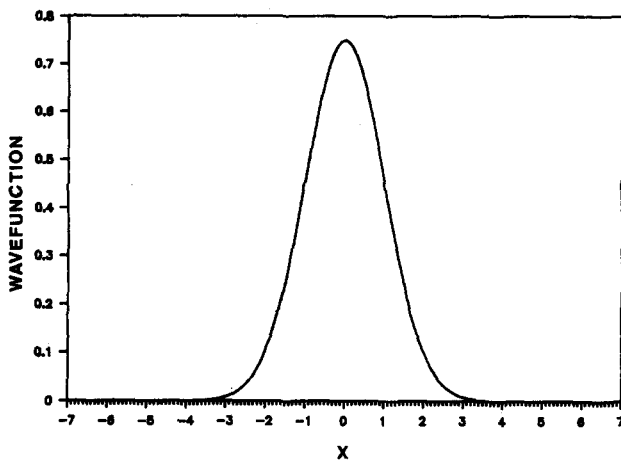


Fig. 1. Magnitude of vacuum, or $|0\rangle$, state versus position.

The contribution from the operators $\hat{a}\hat{a}$ and $\hat{a}^+\hat{a}^+$ is zero because they give terms proportional to $|n-2\rangle$ and $|n+2\rangle$, which are orthogonal to $\langle n|$. So we obtain

$$\langle x^2 \rangle = \langle n | [(2n+1)/2] | n \rangle = n + \frac{1}{2}. \quad (21)$$

The result for $\langle p^2 \rangle$ is the same, so with $\langle x \rangle = \langle p \rangle = 0$, we find, for number states,

$$\text{var}(x) = \text{var}(p) = n + \frac{1}{2}. \quad (22)$$

The product of the number state variances is

$$\text{var}(x) \text{var}(p) = (n + \frac{1}{2})^2, \quad (23)$$

which expresses the Heisenberg uncertainty principle for the oscillator number states. The vacuum state, $n=0$, has the smallest uncertainty product of all the number states, $\frac{1}{4}$, and is said to be a *minimum-uncertainty state*. And because the vacuum state, like all number states, has zero average position and zero average momentum, it is a stationary, minimum-uncertainty wave packet with constant width, as is illustrated in Fig. 1.

III. LINEAR COMBINATION STATES

The number states form a complete orthonormal set, so the most general state imaginable is a linear combination of the number states with time-dependent coefficients. We can write such a state as

$$\psi(x,t) = \sum_{n=0}^{\infty} c_n(t) |n\rangle, \quad (24)$$

where $c_n(t)$ are complex numbers and the number states $|n\rangle$ contain the x dependence.

The time evolution of the complex expansion coefficients $c_n(t)$ is governed by Schrödinger's equation,

$$i \frac{d\psi(x,t)}{dt} = \hat{H}\psi(x,t), \quad (25)$$

where the Hamiltonian operator \hat{H} for the harmonic oscillator is found by writing its classical total energy in terms of x and p and then replacing x and p by their operators. From Eqs. (15) and (16), we obtain

$$\begin{aligned} \hat{H} &= \hat{x}^2/2 + \hat{p}^2/2 = (\hat{a}\hat{a}^+ + \hat{a}^+\hat{a})/2 \\ &= \hat{a}^+\hat{a} + \frac{1}{2} = n + \frac{1}{2}, \end{aligned} \quad (26)$$

so the effect of the Hamiltonian operator operating on a general term, $c_n(t) |n\rangle$ on the right side of (24) is simply to

multiply it by $n + \frac{1}{2}$. That is,

$$\hat{H}c_n(t) |n\rangle = (n + \frac{1}{2})c_n(t) |n\rangle. \quad (27)$$

Substituting from (27) into the Schrödinger equation (25), and equating coefficients term by term, we find a set of *uncoupled* first-order differential equations,

$$i \frac{d}{dt} c_n(t) = \left(n + \frac{1}{2}\right) c_n(t), \quad n = 0, 1, 2, \dots, \quad (28)$$

a general one of which has the solution

$$c_n(t) = c_n(0) e^{-i(n+1/2)t}. \quad (29)$$

It is standard practice to ignore that part of the phase factor, $e^{-i(1/2)t}$, which is common to all of the coefficients. With that convention, each coefficient rotates clockwise in the complex plane at a rate proportional to its n value. The physical significance of each c_n is that its squared magnitude represents the probability of measuring n quanta in the oscillator; these probabilities are seen to be independent of time.

We show next that the annihilation and creation operators are analogous to the classical *phasors*, Ae^{-it} and A^*e^{it} , used to describe a real sinusoidal oscillation at unit angular frequency. To make this connection between classical and quantum worlds, consider the quantum representation of the average position $\langle x \rangle$ of an ensemble of oscillators represented by a general state $|\psi\rangle$. The two terms $\langle \psi | \hat{a}/\sqrt{2} | \psi \rangle$ and $\langle \psi | \hat{a}^+/\sqrt{2} | \psi \rangle$ evaluate as follows at some general time t . First, we operate with \hat{a} on the ket:

$$\begin{aligned} \hat{a}|\psi\rangle &= \hat{a} \sum_{n=0}^{\infty} c_n(0) e^{-int} |n\rangle \\ &= \sum_{n=1}^{\infty} c_n(0) e^{-int} \sqrt{n} |n-1\rangle. \end{aligned}$$

Then we take the scalar product with

$$\langle \psi | = \sum_{n=0}^{\infty} c_n^*(0) e^{int} \langle n |$$

to give

$$\langle \psi | \hat{a} | \psi \rangle = e^{-it} \sum_{n=0}^{\infty} \sqrt{n+1} c_n^*(0) c_{n+1}(0). \quad (30)$$

In similar fashion, we find

$$\langle \psi | \hat{a}^+ | \psi \rangle = e^{it} \sum_{n=0}^{\infty} \sqrt{n+1} c_{n+1}^*(0) c_n(0). \quad (31)$$

Using results (30) and (31) in Eq. (17), we find the following general expression for the time dependence of the expectation value of x :

$$\langle x \rangle = \sqrt{2} \text{Re} \left(e^{-it} \sum_{n=0}^{\infty} \sqrt{n+1} c_n^*(0) c_{n+1}(0) \right). \quad (32)$$

This expectation value is real, as it must be if it is to represent a physical measurement.

Finally, comparing this quantum expression with the corresponding classical phasor representation of a sinusoidally oscillating quantity,

$$\langle x \rangle = 2 \text{Re}(Ae^{-it}), \quad (33)$$

we see that the summation over the coefficients in Eq. (30) [and (31)] provides the quantum analog of the classical phasor amplitude A (and A^*). (Notice that we would have obtained the same time dependence for $\langle x \rangle$ if we had associated an e^{-it} time dependence with the operator \hat{a} and had treated the c_n coefficients as constants in time. This is the

Heisenberg, rather than the Schrödinger, interpretation of quantum mechanics.)

To summarize, *the prescription for going from the classical description of an oscillator to the quantum-mechanical description is simply to replace the classical phasor A by the quantum-mechanical operator \hat{a} or, more precisely, by the bracket $\langle \psi | \hat{a} | \psi \rangle$.*

In the following sections we define particular quantum states to be eigenfunctions of certain operators. Then, with the help of a personal computer, we develop a physical picture of the state as follows. First, we find the specific numerical values of the $c_n(0)$, which define the state uniquely. These values are found from computationally efficient recursion relations that we show how to obtain later on. Beginning with a trial value of $c_0(0) = 1$, the computer calculates higher c_n 's, usually up to $n = 80$, and normalizes them so that $\sum_0^\infty |c_n|^2 = 1$. Then, it calculates the shapes of wave packets, i.e., graphs of ψ (or $|\psi|$) vs x , at various times by using the numerical values of $c_n(0)$ in Eq. (29) to find the $c_n(t)$ and then combining the $c_n(t)$ with the values of the number states at each x from Eqs. (1) and (2).

We have found our computer-generated wave packet graphs to be of enormous help in understanding the properties of various special linear combination states. These special states include coherent states (the subject of Sec. IV), generalized number states, and, of course, squeezed states.

IV. COHERENT STATES

Not every linear combination state is a minimum product state in the sense that $\text{var}(x)\text{var}(p) = \frac{1}{4}$, as occurs for the $|0\rangle$, or vacuum, state. But special sets of $c_n(t)$ that produce minimum product states *do* exist; one such set is known as the *coherent* states. The squeezed states, described in Sec. V, are a more general class of minimum product states.

We define a coherent state $|\alpha\rangle$ to be an eigenfunction of the annihilation operator \hat{a} , with some eigenvalue α (which may be a complex number). That is,

$$\hat{a}|\alpha\rangle = \alpha|\alpha\rangle. \quad (34)$$

Like any other state, a coherent state represented as a linear superposition of number states. Considerable insight into the physical meaning of a coherent state can be obtained by evaluating the coefficients of such a linear superposition. To do so, we substitute the general series expansion [Eq. (24)] into Eq. (34). Thus

$$\hat{a} \sum_{n=0}^{\infty} c_n |n\rangle = \sum_{n=1}^{\infty} c_n \sqrt{n} |n-1\rangle = \alpha \sum_{n=0}^{\infty} c_n |n\rangle. \quad (35)$$

(Here, all the c_n represent their values at $t = 0$.) Now, by matching the coefficients of each number state in the second equality, we can write a set of recursion relations that allows us to evaluate each coefficient in terms of the next lower one:

$$\begin{aligned} c_1 &= \alpha c_0, \\ c_2 &= \alpha c_1 / \sqrt{2}, \\ c_n &= \alpha c_{n-1} / \sqrt{n}. \end{aligned} \quad (36)$$

The general coefficient c_n is expressible in terms of c_0 :

$$c_n = c_0 (\alpha^n / \sqrt{n!}). \quad (37)$$

Using this general expression for the coefficients, we can

evaluate c_0 by imposing the normalization condition,

$$1 = \sum_{n=0}^{\infty} |c_n|^2 = |c_0|^2 \sum_{n=0}^{\infty} (|\alpha|^2)^n / n! = |c_0|^2 e^{|\alpha|^2},$$

which yields

$$|c_0| = e^{-|\alpha|^2/2}. \quad (38)$$

The physical interpretation of a coherent state stems from the fact that $|c_n|^2$ represents the probability P_n of measuring n quanta in the oscillator (or, equivalently, of measuring an energy equal to $n + \frac{1}{2}$). In the case of a coherent state,

$$P_n = |c_n|^2 = e^{-|\alpha|^2} [(|\alpha|^2)^n / n!] = e^{-\langle n \rangle} [\langle n \rangle^n / n!], \quad (39)$$

where we have made the replacement

$$|\alpha|^2 = \langle n \rangle.$$

Equation (39) represents a *Poisson distribution*. That is, P_n is the probability of detecting n independent events in a fixed time interval if $\langle n \rangle = |\alpha|^2$ is the average number of events per time interval. Experimentally, it is found that single mode laser light approximates coherent light and, consequently, has the expected Poisson counting statistics.

So we arrive at the following physical interpretation of a coherent state. *A coherent state $|\alpha\rangle$ is that linear combination of number states whose squared coefficients $|c_n|^2$ represent the probabilities of detecting n quanta in a Poisson distribution with average number of quanta $|\alpha|^2$.* To actually detect the number of photons in a standing light wave, one must let them out of the optical cavity in which they are trapped and let the resulting pulse fall on the cathode of a photomultiplier tube. For example, if one mirror of the cavity is suddenly switched from perfectly reflecting to perfectly transmitting, the light pulses will have a duration or "coherence time" equal to twice the cavity length divided by c . This is the counting time implied in the preceding paragraph. A distribution of counts could be obtained from an ensemble of identically prepared cavities.

To show that a coherent state is indeed a minimum product state, we must calculate the variances of x and p . The details, given in the Appendix, show how straightforward it is to calculate the expectation value of any operator that can be written in terms of the operator for which the state is an eigenfunction. The expectation values of x , p , x^2 , and p^2 for a coherent state $|\alpha\rangle$ are, from the Appendix,

$$\begin{aligned} \langle x \rangle &= \sqrt{2\langle n \rangle} \cos t, \\ \langle p \rangle &= -\sqrt{2\langle n \rangle} \sin t, \\ \langle x^2 \rangle &= 2\langle n \rangle \cos^2 t + \frac{1}{2}, \end{aligned}$$

and

$$\langle p^2 \rangle = 2\langle n \rangle \sin^2 t + \frac{1}{2}. \quad (40)$$

The variances, from Eqs. (3) and (4), are

$$\text{var}(x) = \text{var}(p) = \frac{1}{2}, \quad (41)$$

which yields the minimum product, $\frac{1}{4}$. Notice that the variances are independent of both time and the average number of quanta in the state; *all coherent states are minimum product states with variances equal to those of the vacuum state.*

Unlike the number states, the coherent states are seen to have oscillating expectation values of position and momentum. In fact, the average position $\langle x \rangle$ is seen to lag the average momentum $\langle p \rangle$ by 90° , just as in a classical oscilla-

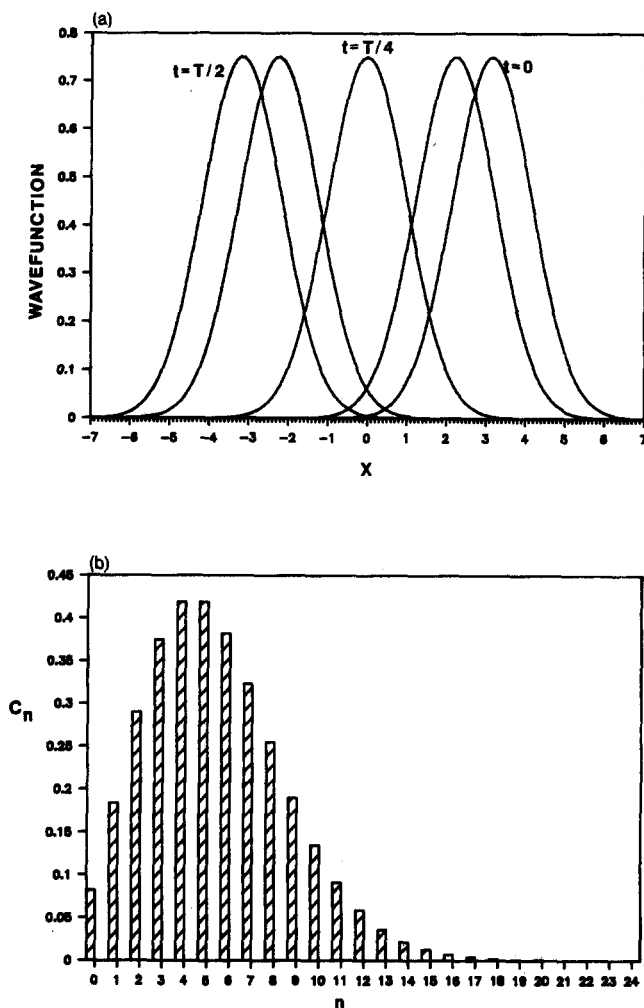


Fig. 2. A coherent state with an average of five quanta. (a) Oscillating wave packet at various times [magnitude of $\psi(x,t)$]. (b) Number state coefficients c_n (at $t = 0$), obtained from recursion relations (36).

tor. Furthermore, the amplitudes of oscillation of $\langle x \rangle$ and $\langle p \rangle$ are proportional to the square root of the average number of quanta, just as those amplitudes in a classical oscillator are proportional to the square root of the oscillator's energy.

Figure 2(a) shows a coherent state wave packet, having an average number of quanta equal to 5.0 at $\frac{1}{2}$ -cycle time intervals.²⁷ The packet has the same Gaussian form as the stationary $|0\rangle$ state wavefunction (see Fig. 1), but it oscillates back and forth along the x axis in the same manner as a classical oscillator. Clearly, the coherent states, not the number states, are the quantum-mechanical analogs of the classical oscillators we observe.

Figure 2(b) is a bar graph of this coherent state's coefficients at time $t = 0$, calculated from the recursion relations of (36). The squares of these coefficients represent the Poisson probabilities of measuring n quanta in the oscillator.

V. SQUEEZED STATES

We have seen that the variances of x and p are independent of time for the number states and for the particular linear combinations of number states that form coherent states. But a general linear combination state has variances

that oscillate sinusoidally in time. This is because the $\cos^2 t$ and $\sin^2 t$ terms in $\langle x^2 \rangle$ and $\langle p^2 \rangle$ in Eq. (40) no longer cancel out when the variances are computed, as they do for a coherent state.

A state is said to be "squeezed" if its oscillating variances become smaller than the variances of the vacuum state. We will see that the product of the variances attains a minimum value only at the instants that one variance is a minimum and the other is a maximum. If the minimum value of the product is equal to $\frac{1}{4}$, then the state is called a minimum-uncertainty squeezed state.

Squeezing is a phenomenon observed experimentally only in special linear combination states produced by some nonlinear process, such as four-wave mixing^{3-7,18,19,28} or parametric amplification.⁸⁻¹⁰ As we discuss in Sec. VII, one can use homodyne detection²⁹⁻³² to measure the quadrature of the squeezed signal in which the noise has been reduced, thereby producing, in principle, a virtually noise-free measurement.

Ignoring for the moment the experimental challenges of producing squeezed states, we will show that it is straightforward to write down linear combinations of number states that show squeezing. Suppose, for example, we want to represent some general $f(x,t)$ by a linear combination of number states. And suppose further that we want this function to have some particular "shape," say, a very narrow pulse, at $t = 0$. Then, to find a particular coefficient $c_n(0)$ in the linear expansion,

$$f(x,0) = c_0(0)|0\rangle + c_1(0)|1\rangle + \cdots, \quad (42)$$

we multiply both sides by $\langle n|$ and carry out the integration over x . Because the number states are orthogonal to one another (and normalized), the rhs reduces to the single number $c_n(0)$ so that

$$\langle n|f(x,0)\rangle = \int_{-\infty}^{\infty} \psi_n^*(x) f(x,0) dx = c_n(0). \quad (43)$$

In this way, one could compute the initial values of the coefficients for any initial shape, provided the integral converges. Once the $c_n(0)$ are computed, one can find the $c_n(t)$ from Eq. (29) and then multiply them by the time-independent number states [Eq. (1)] to find the explicit time and position dependence of the wave packet.

The wave packets that result from this process must obey the uncertainty principle at every instant of time. If, for example, at $t = 0$, we choose an $f(x,0)$ with a small $\text{var}(x)$, then $\text{var}(p)$ at that instant will be at least as large as $1/[4 \text{var}(x)]$. We will see that the shape that leads to a minimum-uncertainty squeezed state is a Gaussian pulse.

But rather than computing squeezed-state coefficients via Eq. (43), we shall now demonstrate another way of finding the coefficients, one that leads directly to minimum-uncertainty squeezed states.

We will show in Sec. VI that a quite general property of a nonlinear device is to create negative and positive frequency output phasors B and B^* that are each linear combinations of the input phasors A and A^* . That is,

$$B = \mu A + \nu A^*$$

and

$$B^* = \mu^* A^* + \nu^* A, \quad (44)$$

where μ and ν are complex numbers. Then, by the general correspondence between classical phasors and annihilation and creation operators discussed in Sec. III, we can write

the following quantum-mechanical operators to represent these output phasors:

$$\begin{aligned}\hat{b} &= \mu \hat{a} + \nu \hat{a}^\dagger \\ \text{and} \\ \hat{b}^\dagger &= \mu^* \hat{a}^\dagger + \nu^* \hat{a}.\end{aligned}\quad (45)$$

Now, recalling that an input coherent state is an eigenfunction of \hat{a} , we might expect the output state to be an eigenfunction of \hat{b} . The eigenfunctions of \hat{b} are squeezed states; they were called two-photon coherent states by Yuen² and were studied extensively by him and by Stoler.³³ But, instead of following their highly mathematical approach, we will attempt to develop a physical understanding of these squeezed states and discover their statistical properties by precisely the same method we used for the coherent states, namely, by writing them as linear combinations of number states and then finding recursion relations that define the coefficients.

If a squeezed state $|\beta\rangle$ is to be an eigenfunction of \hat{b} with eigenvalue β , then

$$\hat{b}|\beta\rangle = \beta|\beta\rangle$$

or

$$(\mu a + \nu a^\dagger) \sum_{n=0}^{\infty} c_n |n\rangle = \beta \sum_{n=0}^{\infty} c_n |n\rangle. \quad (46)$$

Here, the c_n represent the number state coefficients for the squeezed state at $t=0$. Operating term by term with $\mu \hat{a} + \nu \hat{a}^\dagger$ we have,

$$\begin{aligned}\mu \sum_{n=1}^{\infty} \sqrt{n} c_n |n-1\rangle + \nu \sum_{n=0}^{\infty} \sqrt{n+1} c_n |n+1\rangle \\ = \beta \sum_{n=0}^{\infty} c_n |n\rangle.\end{aligned}\quad (47)$$

And finally, by equating coefficients of each number state, we obtain the desired recursion relations:

$$\begin{aligned}c_1 &= \beta c_0 / \mu, \\ c_2 &= (\beta c_1 - \nu c_0) / \mu \sqrt{2}, \\ \text{and, in general,}\end{aligned}\quad (48)$$

$$c_n = \frac{\beta c_{n-1} - \nu \sqrt{n-1} c_{n-2}}{\mu \sqrt{n}}.$$

For a given set of numerical values of μ , ν , and β , we can begin with an arbitrary value of c_0 and find the numerical values of the rest of the coefficients recursively, just as we did for the coherent states in Sec. IV. The value of c_0 is then adjusted for normalization, i.e., $\sum_{n=0}^{\infty} |c_n|^2 = 1$.

It is clear from an inspection of these recursion relations that there are only two, not three, independent parameters, because the ratios, β/μ and ν/μ , uniquely determine all the coefficients. Therefore, provided $|\mu| > |\nu|$, so that the sequence of c_n converges, we are at liberty to choose $|\mu|^2 - |\nu|^2 = 1$. This particular choice of μ and ν results in $\hat{b}\hat{b}^\dagger - \hat{b}^\dagger\hat{b} = (\mu\hat{a} + \nu\hat{a}^\dagger)(\mu^*\hat{a}^\dagger + \nu^*\hat{a})$

$$- (\mu^*\hat{a}^\dagger + \nu^*\hat{a})(\mu\hat{a} + \nu\hat{a}^\dagger) = 1, \quad (49)$$

which is analogous to the corresponding "commutation relation" for \hat{a} and \hat{a}^\dagger [Eq. (12)].

It is tempting to think of $\hat{b}^\dagger\hat{b}$ as the "number operator" for a squeezed state, but this is incorrect. The expectation value of the number of ordinary quanta n is defined by $\sum_{n=0}^{\infty} n |c_n|^2$, which is equal to $\langle \hat{a}^\dagger \hat{a} \rangle$ for all states by Eq.

(11). But we can interpret $\langle \hat{b}^\dagger \hat{b} \rangle$ as giving the number of "somethings." These somethings are not ordinary quanta; instead, we might call them "generalized quanta." We shall try to explain this concept by describing a set of states called "generalized number states" by Yuen.²

Recall that we could build up the infinite set of ordinary number states by starting with the ordinary $|0\rangle$ state and operating repeatedly with the creation operator \hat{a}^\dagger . In exactly the same way, we can build up the set of generalized number states by starting with the generalized zero state and operating repeatedly with the \hat{b}^\dagger operator. But what is this generalized zero state? The ordinary zero state has the property that \hat{a} operating on it gives zero. By analogy, the generalized zero state has the property that \hat{b} operating on it gives zero. But this is just the squeezed state defined by the recursion relation in (48) with $\beta = 0$! As you can see from those recursion relations all the odd coefficients, c_1 , c_3 , etc., are zero, but c_2 , c_4 , etc., are not zero. We can then compute the coefficients of the generalized one state by operating on the generalized zero state with \hat{b}^\dagger . Now all the even coefficients are zero while, in general, the odd ones are different from zero. Continuing in this way and denoting the m th such generalized number state by $|m\rangle$, we can obtain the state $|m+1\rangle$ from $|m\rangle$ by

$$|m+1\rangle = \hat{b}^\dagger |m\rangle / \sqrt{m+1},$$

just as we can obtain the ordinary number state $|n+1\rangle$ from $|n\rangle$ by operating with $\hat{a}^\dagger / \sqrt{n+1}$ on $|n\rangle$ [Eq. (10)]. Note particularly that the various generalized number states produced by this scheme are already normalized; no further scaling of the coefficients c_n for each state is necessary.

We can now find the average number of ordinary quanta in a generalized number state. For example, we leave the reader to show that the average number of ordinary quanta in the generalized one state is given by $\mu^2 + 2\nu^2 = 2\mu^2 - 1$. (Hint: Use steps 1 and 2 beneath Table I to write $a^\dagger a$ in terms of $\hat{b}^\dagger \hat{b}$. Then operate on the generalized one state and take the scalar product with its Hermitian conjugate.)

When the wave packets represented by the generalized number states are computed and plotted as functions of x , we get a rather startling and wonderful result. The graph of $|\psi(x,t)|$ for any generalized number state has the same shape as the corresponding ordinary number state, but the scale along x oscillates as a function of time. That is, the width, separation between zeros, etc., all oscillate sinusoidally in time. The generalized number states "breathe"!

What is the physical significance of a generalized number state? There is no detector, corresponding to a photo-multiplier tube, for the generalized quanta, and no one has produced a generalized number state experimentally. So

Table I. Comparison of expectation values (μ, ν , and β real).

	Coherent	Squeezed
$\langle x \rangle$	$\sqrt{2} \alpha \cos t$	$\sqrt{2} \beta (\mu - \nu) \cos t$
$\langle p \rangle$	$-\sqrt{2} \alpha \sin t$	$-\sqrt{2} \beta (\mu - \nu) \sin t$
$\langle n \rangle$	α^2	$\beta^2 (\mu - \nu)^2 + \nu^2$
$\text{var}(x)$	$\frac{1}{2}$	$(\mu^2 + \nu^2 - 2\mu\nu \cos 2t)/2$
$\text{var}(p)$	$\frac{1}{2}$	$(\mu^2 + \nu^2 + 2\mu\nu \cos 2t)/2$
$\text{var}(n)$	α^2	$\beta^2 (\mu - \nu)^4 + 2\mu^2 \nu^2$

what is a generalized quantum? Apparently it is just another sort of excitation of the oscillator (or electromagnetic field).

The generalized number states form an orthonormal set, so any state of the oscillator should be expressible as a linear combination of them. For example, any squeezed state, when expressed as a linear combination of generalized number states, has a particularly simple set of coefficients; these are just the coefficients that lead to a Poisson distribution. (The proof is identical to the steps leading up to Eq. (47), with \hat{a} replaced by \hat{b} , $|\alpha\rangle$ replaced by $|\beta\rangle$, and the ordinary number states replaced by the generalized number states.) In other words, if we could build a generalized photon detector, a squeezed state would show up as a Poisson distribution of generalized photons.

The analogy between \hat{a} and \hat{b} , etc., can be used to find the number of generalized quanta in a squeezed state. This is just $\langle \beta | \hat{b}^\dagger \hat{b} | \beta \rangle = \beta^2$. Contrast this result with the average number of ordinary quanta in a squeezed state $\langle \beta | \hat{a}^\dagger \hat{a} | \beta \rangle = \beta^2 (\mu - \nu)^2 + \nu^2$ (see Table I). Thus the number of generalized quanta can be larger or smaller than the number of ordinary quanta depending on the values of μ and ν .

Although generalized number states have not been produced experimentally, squeezed states (eigenfunctions of \hat{b}) have been, and we devote the rest of our discussion to them. Figure 3(a) illustrates the oscillating wave packet for a squeezed state with $\mu = 1.5$, $\nu = (\mu^2 - 1)^{1/2} = 1.118$, $\beta = 3$. This packet has an oscillating width, but it is a *minimum-uncertainty packet* because, at $t = \text{integral multiples of } T/4$, the product of the variances of x and p is $\frac{1}{4}$ just as for a coherent state. The variances of a squeezed state actually oscillate in time between $(\mu + \nu)^2/2$ and $(\mu - \nu)^2/2$, completing two oscillations in one oscillator period [see Fig. 3(c) and Table I]. Strong squeezing is indicated by the fact that the variances dip well below the value of $\frac{1}{4}$, the variances of the vacuum state.

Table I shows the expectation values of displacement, momentum, and number of quanta, along with their variances, both for the coherent states and for the squeezed states (for the special case of β , μ , and ν all real). Notice that $\langle n \rangle$ represents the number of ordinary quanta. The number of generalized quanta in a squeezed state is β^2 , as noted above.

The squeezed-state formulas in the table are most easily derived by the following procedure.

(1) Write the appropriate operator in terms of \hat{b} and \hat{b}^\dagger , i.e., as $f(\hat{b}, \hat{b}^\dagger)$, by solving Eq. (45) for \hat{a} and \hat{a}^\dagger in terms of \hat{b} and \hat{b}^\dagger .

(2) Use the commutation relation in the form $\hat{b}\hat{b}^\dagger = \hat{b}^\dagger\hat{b} + 1$ as many times as is necessary to move all \hat{b}^\dagger 's in each term to the left of all \hat{b} 's. The result is called the normally ordered form.

(3) Use the eigenvalue equation, $\hat{b}|\beta\rangle = \beta|\beta\rangle$, and its Hermitian adjoint, $\langle\beta|\hat{b}^\dagger = \beta^*\langle\beta|$, to evaluate the expectation value $\langle\beta|f(\hat{b}, \hat{b}^\dagger)|\beta\rangle$.

The squeezed-state wave packet shown in Fig. 3 has its minimum variance at the positions of maximum displacement. Can we also find squeezed states for which the minimum variance occurs at zero displacement, or perhaps at some arbitrary point in the cycle? Yes, we can, just by changing the relative phase of the complex numbers μ and ν . Figure 4 shows a wave packet for the case $\beta = 0.5$, $\mu = 1.5$, $\nu = -1.118$. The extrema of $\text{var}(x)$ are the same as for the wave packet in Fig. 3, but the minimum variance

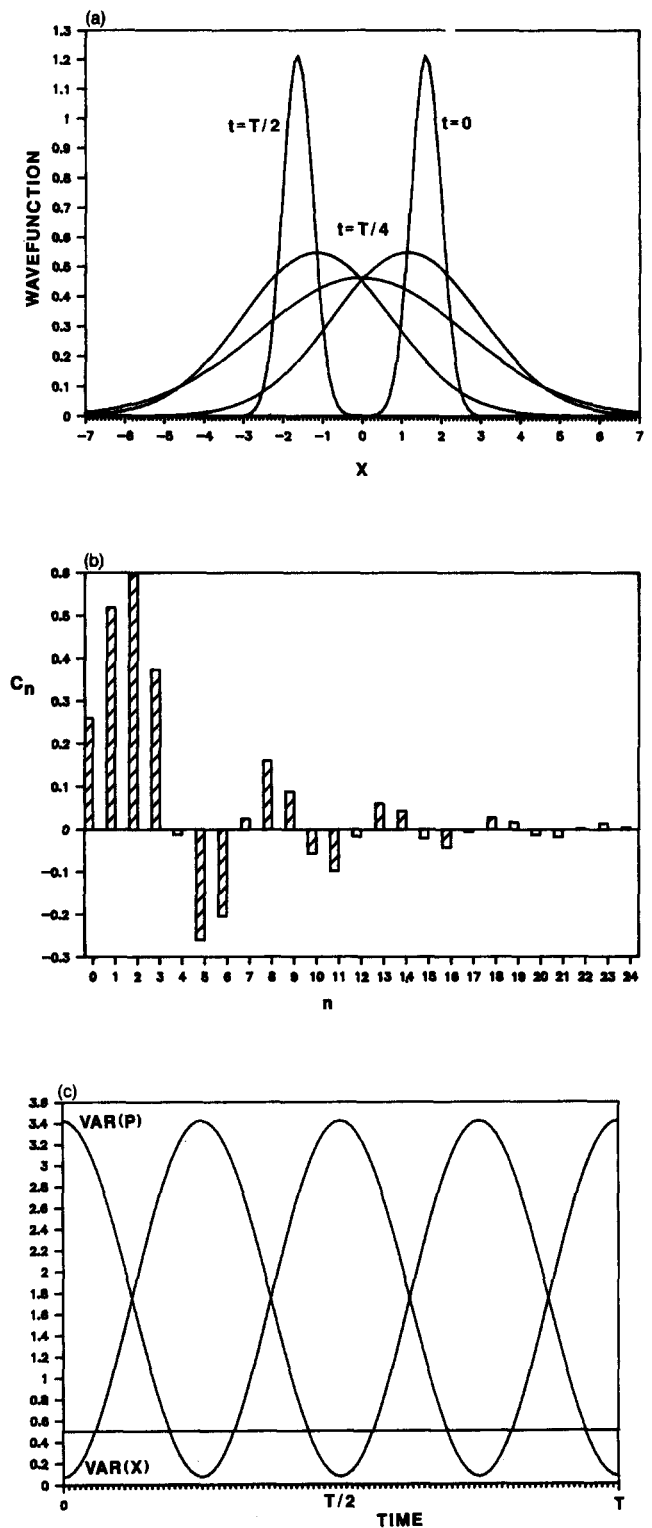


Fig. 3. Squeezed state, an eigenfunction of the operator $\mu\hat{a} + \nu\hat{a}^\dagger$ with eigenvalue $\beta = 3.0$ and with $\mu = 1.5$, $\nu = 1.118$. (a) Oscillating minimum-uncertainty wave packet with oscillating variance. Minimum x variance occurs at maximum displacement. (b) Number state coefficients at $t = 0$. (c) Variances of x and p versus time.

occurs at zero displacement in Fig. 4. For cases in which the phase of ν is neither 0° nor 180° the minimum variance occurs at points in the cycle other than at maximum or zero displacement.

Another important property of squeezed states is the re-

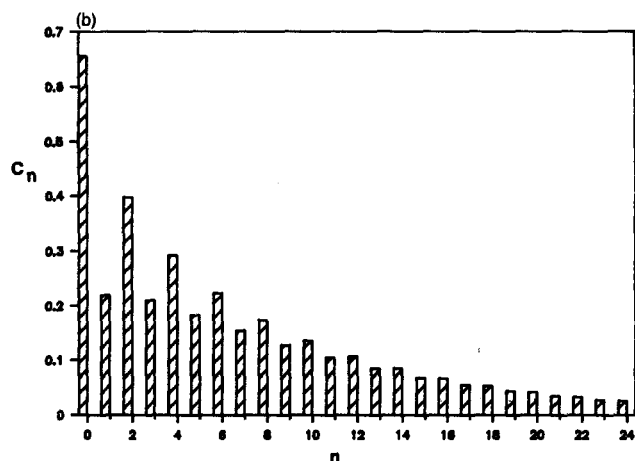
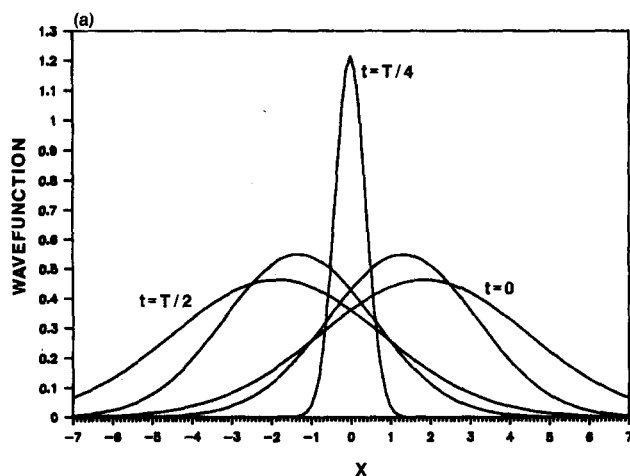


Fig. 4. Squeezed state with $\beta = 0.5$, $\mu = 1.5$, $\nu = -1.118$. (a) Wave packet with minimum x variance at minimum displacement. (b) Number state coefficients.

lation between $\langle n \rangle$ and $\text{var}(n)$. For a coherent state, $\text{var}(n)$ is precisely equal to $\langle n \rangle$, which reflects the fact that the squared coefficients form a Poisson distribution. But, for a squeezed state, $\text{var}(n)$ can be either larger or smaller

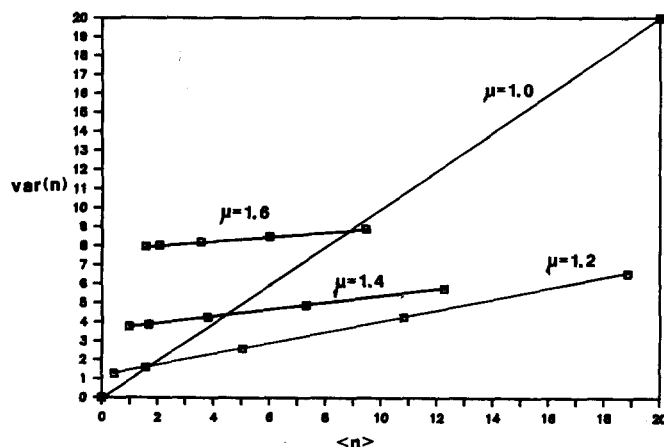


Fig. 5. Variance of number of quanta versus average number of quanta in squeezed states for different amounts of squeezing (μ), with μ and ν both positive. Data points represent $\beta = 0, 2, 4, 6, 8$ for each line.

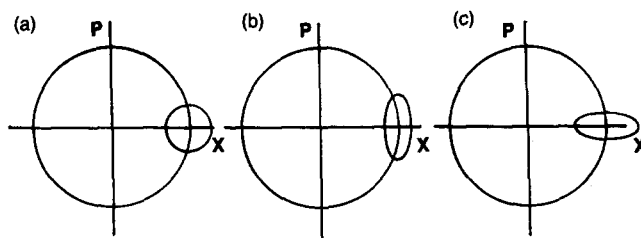


Fig. 6. Phase-space graphs for quantum oscillators, showing uncertainties. (a) Coherent state, equal uncertainties in position and momentum. (b) Squeezed state with minimum $\text{var}(x)$ [or $\text{var}(p)$] occurring when $\langle x \rangle$ (or $\langle p \rangle$) has maximum displacement from zero. (c) Squeezed state with minimum $\text{var}(x)$ [or $\text{var}(p)$] occurring when $\langle x \rangle$ (or $\langle p \rangle$) is zero.

than $\langle n \rangle$. Figure 5 shows how $\text{var}(n)$ depends on $\langle n \rangle$ for four values of μ and for μ and ν each real and positive, as β is varied. The linear relation between $\text{var}(n)$ and $\langle n \rangle$ for fixed μ and ν occurs because $\text{var}(n)$ and $\langle n \rangle$ have the same functional dependence on β (see Table I). The slopes of the straight lines, equal to $(\mu - \nu)^2$, decrease as μ and, therefore, ν increase, while their intercepts on the $\text{var}(n)$ axis increase.

The interesting feature illustrated in Fig. 5 is that for any value of μ greater than 1 and for positive ν , the distribution of quanta always becomes *sub-Poissonian* for a large enough average number of quanta; that is, $\text{var}(n)$ becomes smaller than $\langle n \rangle$. If sub-Poissonian statistics are obtained for the photons in a traveling electromagnetic wave, those photons are said to be "antibunched."^{34,35} In such an antibunched beam the photons are more uniformly spaced in time than the photons in a coherent beam having the same average number of photons per second. The reduction in uncertainty of the number of photons counted in a fixed time interval would reduce the "noise" in any communication system that is based on photon counting.

One's physical intuition regarding the relationship between photon counting statistics and the phases of the variance oscillations relative to the average position oscillations can be enhanced by the phase space (momentum versus displacement) graphs of Fig. 6. These graphs are extensions of the classical phase-space diagram for an oscillator. Classically, an oscillator's phase-space trajectory is a circle (for appropriately normalized variables). In the quantum picture, the instantaneous position and momentum in phase space are blurred by the uncertainty principle. Because the oscillator's average energy is [from Eq. (26)] proportional to the average square of the radius vector in phase space and to its average number of quanta (plus $\frac{1}{2}$), we see that the oscillator states represented by the rotating blur have uncertainties in their energy and in their number of quanta.

Figure 6(a) represents a coherent state, for which the uncertainties in position and momentum are equal as suggested by the error circle. We saw earlier that the counting statistics are *Poissonian* for a coherent state. Figure 6(b) shows a squeezed state of the type shown in Fig. 3, the minimum of $\text{var}(x)$ at maximum displacement, as suggested by the error ellipse with its major axis always tangent to the phase-space trajectory. For this case, the radius vector is also squeezed, which accounts for the possibility of *sub-Poissonian* statistics. But, in Fig. 6(c), which shows a squeezed state with the major axis of the error ellipse always in the radial direction, we have an example of *super-*

Poissonian statistics [$\text{var}(n)$ greater than $\langle n \rangle$]. For example, for the case shown in Fig. 4, Table I yields the values $\langle n \rangle = 2.96$, $\text{var}(n) = 17.39$.

VI. GENERATION OF A SQUEEZED OPTICAL STATE

To date, attempts to produce squeezed states at optical frequencies have involved either parametric amplification or four-wave mixing. Both of these processes involve nonlinear interactions, in which a weak signal wave is mixed with (multiplied by) a strong "pump" wave. The result is an output wave that typically contains a rich mixture of harmonics and sum and difference frequencies. Both parametric amplification and four-wave mixing are phase-sensitive processes, which means that the amplitude of the output wave depends on the relative phase of the signal and pump. Generally, if an input wave at some relative phase θ is maximally amplified, then an input wave in the opposite quadrature (phase shifted by $\pm \pi/2$ rad) will be maximally attenuated.

In the case of degenerate parametric amplification, the inputs to the nonlinear device are a weak signal wave at angular frequency ω and a strong pump wave at angular frequency 2ω . Each of these real waves, representing oscillating electric and magnetic fields, can be composed of positive and negative frequency phasors. Multiplication of the positive frequency input signal phasor $A * e^{i\omega t}$ by the negative frequency pump phasor $P e^{-2i\omega t}$ gives a contribution to the output proportional to $A * P e^{-i\omega t}$. At the same time, multiplication of the negative frequency input signal phasor $A e^{-i\omega t}$ by $P * e^{2i\omega t}$ and by $P e^{-2i\omega t}$ produces a contribution to the output proportional to $A P P * e^{-i\omega t}$. In general, the magnitude of the negative frequency output phasor $B e^{-i\omega t}$ is a linear combination of the positive and negative frequency input signal phasors,

$$B = \mu A + \nu A^*, \quad (50)$$

where the relative phase of the A and A^* contributions is determined by the phases of μ and ν .

In the case of degenerate four-wave mixing, the signal and pump input waves are both at angular frequency ω . At optical frequencies two strong, counterpropagating pump beams are usually introduced at a slight angle with respect to the weak signal beam. The nonlinearity involves the polarization Q of the medium and the driving electric field E , for example,

$$Q = k_1 E + k_3 E^3 + \text{higher-order terms.} \quad (51)$$

The cubic term can mix the positive frequency signal phasor $A * e^{i\omega t}$ down to a negative frequency via the product, $A * e^{i\omega t} P e^{-i\omega t} P e^{-i\omega t}$, while the negative frequency signal contributes to the negative frequency output phasor via both the linear term and the product $A e^{-i\omega t} P e^{-i\omega t} P * e^{i\omega t}$ from the cubic term.

We are now in a position to understand, in a completely classical way, how the phase-sensitive nature of parametric amplification or four-wave mixing can lead to squeezing. Consider the ensemble of oscillators represented by the blur circle of Fig. 6(a). If, by a nonlinear process, the component of each phasor that lies parallel to the x axis at the instant shown is attenuated, while the component that lies along the p axis is amplified, then we get the situation in part (b) of the figure. On the other hand, if the component of each phasor along the x axis is amplified, while the com-

ponent along the p axis is attenuated, then we arrive at the situation in part (c).

The process of squeezing is now seen to be a classical phenomenon, based on phase-sensitive amplification. If there is a signal present at the input of the squeezing device, both signal and noise (whether the noise is of thermal origin or is due to the fundamental quantum uncertainties) are amplified in one quadrature and attenuated in the other quadrature. The signal-noise ratio in each quadrature remains the same.

VII. HOMODYNE DETECTION OF SQUEEZED STATES

One might question the usefulness of a measurement whose variance oscillates rapidly between a very low and a very high value. We show next that it is possible to measure a physical variable having a squeezed variance that is constant in time.

The conversion of an oscillating quantity to a constant quantity has a long and honorable history in physics and engineering. The method, called *homodyne detection* or *phase-sensitive detection*, involves multiplication of the oscillating signal by a "local oscillator" wave at exactly the same frequency as the signal, followed by time averaging or, equivalently, low-pass filtering. (In the closely related *heterodyne detection* method, the signal and local oscillator frequencies are different.) The product of the signal and local oscillator can have a nonzero average value proportional to the signal amplitude, as well as an oscillating component at twice the signal frequency, which can be removed by time averaging.

We begin our analysis in the classical domain, representing the sinusoidal signal, the displacement of the oscillator, by

$$x(t) = x_0 e^{-i\omega t} + x_0^* e^{i\omega t} \quad (52)$$

and the local oscillator wave by

$$y(t) = y_0 e^{-i(\omega t + \theta)} + y_0^* e^{i(\omega t + \theta)}. \quad (53)$$

Here, we have used the subscript to emphasize that x_0 , x_0^* , $y_0 e^{-i\theta}$, and $y_0^* e^{i\theta}$ represent the rotating phasors at time $t = 0$ and that all four entities are, therefore, constant complex numbers. (The phase θ of the local oscillator is shown explicitly because it usually can be adjusted by the experimenter.) The product,

$$x(t)y(t) = x_0 y_0 e^{i\theta} + x_0^* y_0 e^{-i\theta} + x_0 y_0^* e^{-i(2\omega t + \theta)} + x_0^* y_0^* e^{i(2\omega t + \theta)}, \quad (54)$$

contains constant terms and terms that oscillate at angular frequency 2ω ; the latter disappear when the product is time averaged.

In homodyne detection of a squeezed state, the local oscillator always has much greater amplitude than the signal, which means that the fractional fluctuations in x_0 are much larger than the fractional fluctuations in y_0 . As in most treatments of homodyne detection, we will treat y_0 as having no fluctuations at all and, in fact, we will omit the factor y_0 altogether.

The output of a homodyne detector is the time-averaged product d of the signal and local oscillator where, from (54),

$$d = x_0 e^{i\theta} + x_0^* e^{-i\theta}. \quad (55)$$

Although this measured quantity has no inherent time de-

pendence, it does have a quantum-mechanical expectation value $\langle d \rangle$ and a variance $\text{var}(d)$, which, in an actual measurement of detector output versus time, are manifested as an average value plus fluctuations, or noise.

To calculate $\langle d \rangle$ and $\text{var}(d)$, we go to the quantum domain by the now familiar technique of replacing the phasors x_0 and x_0^* with the annihilation and creation operators \hat{a} and \hat{a}^+ . The resulting quantum-mechanical operator \hat{d} represents the detector output d in exactly the same way that the quantum-mechanical operators \hat{x} and \hat{p} represent the classical position and momentum of the oscillator or the electric and magnetic fields of the signal mode.

Making the operator replacements indicated above, we obtain

$$\begin{aligned}\hat{d} &= \hat{a}e^{i\theta} + \hat{a}^+e^{-i\theta} \\ &= \hat{a}(\cos \theta + i \sin \theta) + \hat{a}^+(\cos \theta - i \sin \theta) \\ &= \sqrt{2}(\hat{x} \cos \theta - \hat{p} \sin \theta).\end{aligned}\quad (56)$$

This equation shows that the detector output is proportional to a linear combination of the oscillator's initial position and momentum. Furthermore, by adjusting the local oscillator phase to be 0 or $\pi/2$, one can choose the detector output to be proportional to the initial displacement or proportional to the initial momentum. These are said to be *quadrature* measurements because they involve a quarter-cycle phase shift of the local oscillator and because they measure the magnitudes of two variables, position and momentum, that are a quarter-cycle out of phase in time.

The variance (noise) of the detector output can be made proportional either to the variance of the initial position or to the variance of the initial momentum, depending on the phase setting. And, as long as the phase remains constant, the variance of the detector output remains constant. Indeed, the usual experimental "proof" of squeezing¹⁸ involves looking at the noise output of a homodyne detector and varying the local oscillator phase. If the noise level oscillates with period π as the phase is varied, and if the noise level goes below the vacuum noise level, then squeezing has been demonstrated.

VIII. DISCUSSION

We have shown that squeezed states are analogous to coherent states. Each type is defined to be an eigenfunction of a certain operator: the annihilation operator in the case of the coherent states, a linear mixture of the annihilation and creation operators in the case of the squeezed states. In each case, we developed computationally efficient recursion relations for the number state coefficients in the linear superposition that makes up the state. Then, using definite numerical parameters, we calculated the coefficients and produced graphs of wave packets at various times directly from the number states, whose values at each position x were calculated with the help of the recursion relations for the Hermite polynomials. The oscillations in $\text{var}(x)$ for these wave packets were evident from the graphs, but we also showed how to calculate the expectation values and variances of position and momentum as functions of time by operator methods.

We have seen that squeezed quantum-mechanical states of an oscillator are an entirely predictable extrapolation of the (not unusual) case of oscillating variances when number states are combined. Clearly, states with nonoscillating variances, such as the coherent states, are special cases

among the infinite variety of states, even though they may be easily prepared with a laser. It is a natural, yet profound, idea that one quadrature's variance can be very small, while the other quadrature's variance is large enough to satisfy the uncertainty principle.

We have also discussed, in a semiquantitative way, how nonlinear interactions with a pump wave can mix the classical positive and negative frequency phasors and, by analogy, the creation and annihilation operators. And we have seen how the process of squeezing can be understood classically, as phase-sensitive amplification. On the other hand, we have *not* attempted to make a quantitative connection between an input coherent state and an output squeezed state in such a nonlinear interaction or to establish a photon by photon formalism. Although the calculation of quantum-mechanical amplitudes for various final states when individual photons are incident on a nonlinear device is an unsolved problem, we can expect, from conservation of energy, that the signal photons added to the output must come from the annihilation of pump photons. For example, in a degenerate parametric amplifier the annihilation of one, two, three, etc., pump photons at frequency 2ω would give rise to two, four, six, etc., output signal photons at frequency ω in addition to the stimulating input signal photon.

We have also shown that with homodyne detection, in which squeezed light is mixed with local oscillator light of the same frequency (in practice, the two beams are added with a beam splitter and allowed to fall on a photomultiplier tube cathode or a photo diode), we can "squeeze" most of the uncertainty into the nonmeasured quadrature for as long a time as we wish to measure the signal. This measurement scheme is equivalent to placing ourselves in a rotating reference frame in phase space, in which the variance of the measured quantity is constant.

The essentially numerical methods we have presented for examining squeezed states depend on the computer's ability to keep track of a large number of coefficients. This use of the computer as a bookkeeping device for coefficients can also be applied to situations in which the system Hamiltonian connects two (or more) modes; this is the quantum-mechanical version of the coupled oscillator problem, which is equivalent to treating the pump wave, as well as the signal wave, quantum mechanically. In the coupled oscillator problem, the system wave function can be specified as a linear combination of base states $|n_1, n_2\rangle$ in which one oscillator contains n_1 quanta and the other contains n_2 quanta. The correlations produced between oscillators via interaction terms in the Hamiltonian then permit information about one oscillator to be deduced from measurements on the other oscillator, a situation sometimes described as the Einstein-Podolsky-Rosen (EPR) paradox.^{36,37}

APPENDIX

One way to find the average $\langle x \rangle$, $\langle p \rangle$, $\langle x^2 \rangle$, and $\langle p^2 \rangle$ for an ensemble of oscillators represented by a coherent state is to substitute the general expression for a coherent state coefficient [from (37)] into Eqs. (30) and (31). This is, in fact, how our computer program makes these calculations. But when we can write the operators in terms of the annihilation and creation operators and when the states themselves are coherent states, there is a simpler and more elegant method.

For a coherent state $|\alpha\rangle$, we have $\hat{a}|\alpha\rangle = \alpha|\alpha\rangle$. The Hermitian adjoint of this relation is $\langle\alpha|\hat{a}^\dagger = \alpha^*\langle\alpha|$. At time $t = 0$ the expectation values of \hat{a} and \hat{a}^\dagger are found directly from these eigenvalue equations:

$$\langle\alpha|\hat{a}|\alpha\rangle = \alpha$$

and

$$\langle\alpha|\hat{a}^\dagger|\alpha\rangle = \alpha^* \quad (\text{A1})$$

Equations (30) and (31) showed quite generally that these expectation values have a complex exponential time dependence. Therefore, when we combine these expectation values to find the time-dependent expectation values of position and momentum, we obtain

$$\langle x \rangle = \langle\alpha|(\hat{a} + \hat{a}^\dagger)/\sqrt{2}|\alpha\rangle = (\alpha e^{-it} + \alpha^* e^{it})/\sqrt{2}$$

and

$$\langle p \rangle = \langle\alpha|(\hat{a} - \hat{a}^\dagger)/\sqrt{2}i|\alpha\rangle = (\alpha e^{-it} - \alpha^* e^{it})/\sqrt{2}i \quad (\text{A2})$$

For real eigenvalues α , these reduce to

$$\langle x \rangle = \sqrt{2}\alpha \cos t$$

and

$$\langle p \rangle = -\sqrt{2}\alpha \sin t \quad (\text{A3})$$

which are equivalent to the first two of Eqs. (40).

To find $\langle x^2 \rangle$ and $\langle p^2 \rangle$ for a coherent state we must evaluate $\langle\alpha|aa|\alpha\rangle$, $\langle\alpha|a^\dagger a^\dagger|\alpha\rangle$, $\langle\alpha|a^\dagger a|\alpha\rangle$, and $\langle\alpha|aa^\dagger|\alpha\rangle$ [see Eqs. (15) and (16)]. The bracket $\langle\alpha|aa|\alpha\rangle$ is conveniently computed by operating twice on a coherent state with the annihilation operator. Because there are two factors of e^{-it} we find

$$\langle\alpha|aa|\alpha\rangle = \alpha^2 e^{-2it} \quad (\text{A4})$$

The second bracket is the complex conjugate of (A4):

$$\langle\alpha|\hat{a}^\dagger \hat{a}^\dagger|\alpha\rangle = (\alpha^*)^2 e^{2it} \quad (\text{A5})$$

The third bracket evaluates to

$$\langle\alpha|\hat{a}^\dagger \hat{a}|\alpha\rangle = \alpha^* \alpha \quad (\text{A6})$$

The fourth and final bracket is first converted to "normal order" (all creation operators to the left of all annihilation operators) by using the commutation relation [Eq. (12)], and then reduced by the eigenvalue equations

$$\begin{aligned} \langle\alpha|\hat{a}^\dagger \hat{a}|\alpha\rangle &= \langle\alpha|\hat{a}^\dagger \hat{a} + 1|\alpha\rangle \\ &= \alpha^* \alpha + 1 \end{aligned} \quad (\text{A7})$$

Combining Eqs. (A4) through (A7) according to Eqs. (15) and (16), we obtain (for real α),

$$\begin{aligned} \langle x^2 \rangle &= [\alpha^2(e^{2it} + e^{-2it}) + 2\alpha^2 + 1]/2 \\ &= \alpha^2(1 + \cos 2t) + 1/2 \\ &= 2\alpha^2 \cos^2 t + 1/2, \end{aligned} \quad (\text{A8})$$

and

$$\begin{aligned} \langle p^2 \rangle &= [-\alpha^2(e^{2it} + e^{-2it}) + 2\alpha^2 + 1]/2 \\ &= \alpha^2(1 - \cos 2t) + 1/2 \\ &= 2\alpha^2 \sin^2 t + 1/2. \end{aligned} \quad (\text{A9})$$

Equations (A8) and (A9) are equivalent to the last two equations of (40) in the text.

¹D. F. Walls, *Nature* **306**, 141 (1983).

²H. P. Yuen, *Phys. Rev. A* **13**, 2226 (1976).

³H. P. Yuen and J. H. Shapiro, *Opt. Lett.* **4**, 334 (1979).

⁴G. J. Milburn, D. F. Walls, and M. D. Levenson, *J. Opt. Soc. Am. B* **1**, 390 (1984).

⁵M. D. Levenson, R. M. Shelby, and S. H. Perlmuter, *Opt. Lett.* **10**, 514 (1985).

⁶M. D. Levenson, R. M. Shelby, M. D. Reid, D. F. Walls, and A. Aspect, *Phys. Rev. A* **32**, 1550 (1985).

⁷R. M. Shelby, M. D. Levenson, D. F. Walls, A. Aspect, and G. J. Milburn, *Phys. Rev. A* **33**, 4008 (1986).

⁸B. Yurke, *Phys. Rev. A* **29**, 408 (1984).

⁹H. J. Carmichael, G. J. Milburn, and D. F. Walls, *J. Phys. A* **17**, 469 (1984).

¹⁰G. J. Milburn and D. F. Walls, *Opt. Commun.* **39**, 401 (1981).

¹¹M. D. Reid, D. F. Walls, and B. J. Dalton, *Phys. Rev. Lett.* **55**, 1288 (1985).

¹²G. J. Milburn, *Opt. Acta* **31**, 671 (1984).

¹³G. J. Milburn, *J. Phys. A* **17**, 737 (1984).

¹⁴R. A. Fischer, M. M. Nieto, and V. D. Sandberg, *Phys. Rev. D* **29**, 1107 (1984).

¹⁵*Phys. Today* **39** (3), 17 (1986).

¹⁶R. L. Robinson, *Science* **230**, 927 (1985).

¹⁷R. L. Robinson, *Science* **233**, 280 (1986).

¹⁸R. E. Slusher, L. W. Hollberg, B. Yurke, J. C. Mertz, and J. F. Valley, *Phys. Rev. Lett.* **55**, 2409 (1985).

¹⁹R. M. Shelby, M. D. Levenson, S. H. Perlmuter, R. G. DeVoe, D. F. Walls, *Phys. Rev. Lett.* **57**, 691 (1986).

²⁰C. M. Caves, *Phys. Rev. D* **23**, 1693 (1981).

²¹H. P. Yuen and J. H. Shapiro, *IEEE Trans. Inf. Theory* **IT-24**, 657 (1978).

²²J. H. Shapiro, H. P. Yuen, and J. A. Machado Mata, *IEEE Trans. Inf. Theory* **IT-25**, 179 (1979).

²³For example, W. H. Louisell, *Quantum Statistical Properties of Radiation* (Wiley, New York, 1973), Sec. 4.3.

²⁴R. J. Glauber, *Phys. Rev.* **131**, 2766 (1963).

²⁵For example, L. I. Schiff, *Quantum Mechanics* (McGraw-Hill, New York, 1949), Chap. IV.

²⁶P. A. M. Dirac, *Quantum Mechanics* (Oxford U.P., London, 1947), 3rd ed., Chap. VI.

²⁷In Figs. 1-4, the numerical values of number states $|0\rangle$ through $|80\rangle$ were generated from Eqs. (2) and (3) at 141 values of x from $x = -7.0$ to $x = 7.0$ at intervals of 0.1. To obtain the wavefunction at each x and t , the value of each number state at that position was multiplied by the appropriate numerical coefficient $c_n(0)e^{-int}$ of that number state, and the series summed. All calculations were performed on a personal computer containing an Intel 8087 math coprocessor with a program written in the PASCAL language.

²⁸D. M. Pepper, *Opt. Eng.* **21**, 156 (1982).

²⁹H. P. Yuen and V. W. S. Chan, *Opt. Lett.* **8**, 177 (1983).

³⁰B. L. Schumaker, *Opt. Lett.* **9**, 189 (1984).

³¹J. H. Shapiro, *IEEE J. Quantum Electron.* **QE-21**, 237 (1985).

³²B. Yurke, *Phys. Rev. A* **32**, 311 (1985).

³³D. Stoler, *Phys. Rev. D* **1**, 3217 (1970); **4**, 1925 (1971).

³⁴D. Stoler, *Phys. Rev. Lett.* **33**, 1397 (1974).

³⁵H. Paul, *Rev. Mod. Phys.* **54**, 1061 (1982).

³⁶A. Einstein, D. Podolsky, and N. Rosen, *Phys. Rev.* **47**, 777 (1935).

³⁷N. D. Mermin, *Phys. Today* **38** (4), 38 (1985).